



# A precise curved motion planning for a differential driving mobile robot

Soonshin Han, ByoungSuk Choi, JangMyung Lee \*

Department of Electronics Engineering, Pusan National University, Pusan 609-735, Republic of Korea

## ARTICLE INFO

### Article history:

Received 24 April 2006

Accepted 2 April 2008

### Keywords:

Differential driving mobile robot

Single curvature

Path planning

Tracking error

## ABSTRACT

A single curvature trajectory with a fixed rotation radius is proposed for an optimal trajectory plan for a differential driving mobile robot to capture a moving object. Generally, when the differential driving mobile robot moves along a path whose rotation radius is not constant, the tracking error of the mobile robot increases with the travel distance. Also, tracking errors increase greatly when the mobile robot follows a trajectory, with a small rotation radius. Based on these two observations, a single curvature trajectory, which has a constant and large rotation radius, is proposed as an optimal trajectory, in order to minimize the tracking error of the differential driving mobile robot. This paper first reviews the characteristics of a single curvature trajectory. Next, an algorithm to capture a moving object precisely is proposed using the single curvature trajectory. With the pre-determined initial states (i.e., position and orientation of the mobile robot and the final states), the mobile robot is made to capture a moving object. Through simulations and real experiments using a two DOF wheel-based mobile robot, the effectiveness of the proposed algorithm is verified.

© 2008 Elsevier Ltd. All rights reserved.

## 1. Introduction

Research on mobile robots can be globally classified into three categories: path planning [1–3], position estimation [4–6], and driving control [7–9]. The trajectory planning of a mobile robot aims at providing an optimal path from an initial position to a target position [10]. Optimal trajectory planning for a mobile robot provides a path, which has minimal tracking error and the shortest driving time and distance.

Tracking errors of mobile robots cause collisions with obstacles due to deviations from the planned path and also cause the robot to fail to accomplish the mission successfully. Tracking error can be reduced through feedback control. However, this requires excessive control efforts due to high control gains. Tracking errors also cause an increase of traveling time, as well as travel distance, due to the additional adjustments needed to satisfy the driving states. Therefore, trajectory planning to decrease tracking error is very important and needs to be handled carefully [11].

One of the major reasons for tracking error is the discontinuity of the rotation radius on the path of the differential driving mobile robot. The rotation radius changes at the connecting point of the straight line route and curved route, or at a point of inflection. At these points, it can be easy for the differential driving mobile robot to secede from its determined orbit due to the rapid change of direction [12]. Therefore, in order to decrease tracking error, the trajectory of the mobile robot must be

planned so that the rotation radius is maintained at a constant, if possible.

The increase of tracking error due to the small rotation radius interferes with the accurate driving of the mobile robot. The path of the mobile robot can be divided into curved and straight-line segments, globally. While tracking error is not generated in the straight-line segment, significant error is produced in the curved segment due to centrifugal and centripetal forces, which cause the robot to slide over the surface. Also, tracking error increases when the rotation radius is small. In fact, the straight line segment can be considered as a curved segment whose rotation radius is infinity. As the tracking error becomes larger at the curved segment, the possibility of a tracking error increases with the decrease of the rotation radius of the curved path. Note that a relatively small error occurs at the straight-line path.

Therefore, it is important to maintain simultaneously a large and constant rotation radius in order to decrease the tracking error of the differential driving mobile robot. This paper proposes a single-curvature trajectory, which has a constant and large rotation radius. In view of the size and discontinuity of the rotation radius, a single-curvature trajectory and a double-curvature trajectory are compared to show that the tracking error increases with the decrease of the rotation radius. Through the tracking experiments along each trajectory, it is proved that a single-curvature trajectory has the least tracking error. With precise trajectory planning, an algorithm for the mobile robot to capture a moving object is proposed. With the pre-specified initial position and orientation of a mobile robot and the final states, and assuming that the velocity of the moving object is pre-estimated, an optimal

\* Corresponding author. Tel.: +82 51 510 2378; fax: +82 51 514 1693.

E-mail address: [jmlee@pusan.ac.kr](mailto:jmlee@pusan.ac.kr) (J. Lee).

capturing path of a mobile robot is produced as a result of this research.

In Section 2, the driving characteristics of a mobile robot are analyzed using a kinematics analysis while the mobile robot is making curved motions. The single-curvature trajectory and double-curvature trajectory are described in detail in Section 3. In Section 4, a curved trajectory formation algorithm, according to a single-curvature trajectory, is introduced with theoretical formulas. Section 5 shows a comparison between a single-curvature and a double-curvature trajectory, with respect to tracking error, in real capturing experiments. Section 6 concludes this paper and provides an agenda for future work.

## 2. Moving characteristics of a differential driving mobile robot

To form a trajectory for a differential driving mobile robot, a kinematics analysis first needs to be conducted. Based on the kinematics analysis, the driving characteristics of a mobile robot with a differential driving mechanism are modeled, which provides the theoretical basis for trajectory planning.

### 2.1. Kinematics analysis of the mobile robot

As shown in Fig. 1a, a mobile robot with a differential driving mechanism has two wheels on the same axis, and each wheel is controlled by an independent motor. Let us define  $v_L$  as the velocity of the left wheel,  $v_R$  as that of the right wheel, and  $l$  as the distance between the two wheels. The robot's motion can be determined by the two wheel velocities,  $v_L$  and  $v_R$ , and the linear and angular velocities,  $v_I$  and  $v_w$ , of the mobile robot can be described in terms of  $v_L$  and  $v_R$  as follows [13]:

$$v_I = \frac{v_R + v_L}{2} \quad (1)$$

$$v_w = \frac{2(v_R - v_L)}{l} \quad (2)$$

A kinematics model of a mobile robot with a differential driving mechanism can be described as shown in Fig. 1b.

In two-dimensional  $X - Y$  Cartesian coordinates, the position of the mobile robot is described by  $x_R(t)$  and  $y_R(t)$ , whereas the orientation is represented as  $\theta_R(t)$ . Then,  $\dot{x}_R(t)$  and  $\dot{y}_R(t)$  represent the linear velocities, whereas  $\dot{\theta}_R(t)$  represents the angular velocity. The velocity vector of the mobile robot is defined as

$$\dot{P} = [\dot{x}_R \quad \dot{y}_R \quad \dot{\theta}_R]^T, \quad (3)$$

where  $P = [x_R \quad y_R \quad \theta_R]^T$ .

Now, the kinematics model of the mobile robot can be represented as [14]

$$\begin{bmatrix} \dot{x}_R \\ \dot{y}_R \\ \dot{\theta}_R \end{bmatrix} = \begin{bmatrix} \cos \theta_R & 0 \\ \sin \theta_R & 0 \\ 0 & 1 \end{bmatrix} \begin{bmatrix} v_1 \\ v_2 \end{bmatrix}. \quad (4)$$

### 2.2. Driving principle of the mobile robot

Through the kinematics analysis, it can be recognized that the motion states of a mobile robot with a differential driving mechanism change according to the velocities of the two wheels. When a robot with multiple wheels rotates about a rotation center instantaneously, this rotation center is defined as the ICC (Instantaneous Center for Curvature). As shown in Fig. 2a, the ICC is located at the cross-section point of the extension-lines of the wheel centers. For a mobile robot with a differential driving mechanism, as shown in Fig. 2b, the ICC can be located at any point on the wheel axis, since the two wheel axes are on the same line. In this case, the ICC will be determined by the velocity ratio between the two wheels.

Fig. 3 illustrates the ICC along with the robot's motion and position. There is a proportional relationship between the wheel velocities and the distance from the wheel to the ICC, which is represented as

$$v_L : v_R = R - \frac{l}{2} : R + \frac{l}{2}. \quad (5)$$

In addition, Eq. (5) can be simply represented as [15]

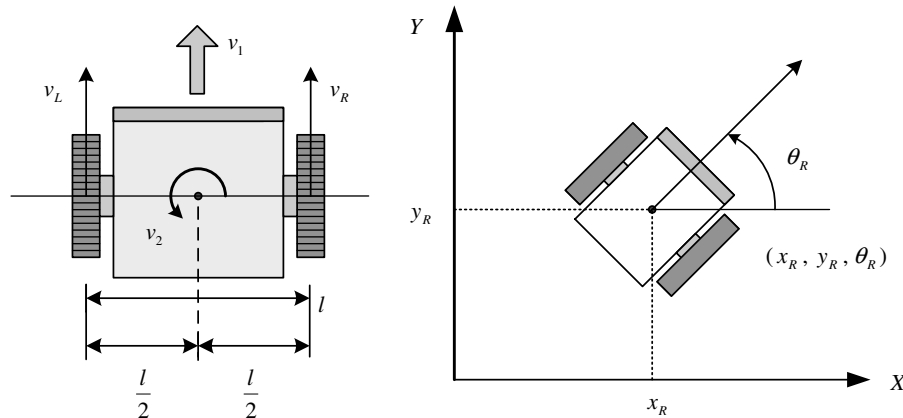
$$R = \frac{l}{2} \left( \frac{v_R + v_L}{v_R - v_L} \right). \quad (6)$$

Note that the rotation radius of the mobile robot is determined by the values of the left and right wheel velocities. When the robot is following a straight line,  $R = \infty$  and  $v_R = v_L$ . When  $v_R \neq v_L$ , the robot follows a curved trajectory of a certain rotation radius. Therefore, the velocity and acceleration of the robot is changed if the rotation radius is varied.

When the mobile robot is moving from A, where the robot is located on  $(x_R, y_R, \theta_R)$  at time  $t$ , to B, where the position is  $(x'_R, y'_R, \theta'_R)$  at time  $t + \delta t$ , the coordinates of the ICC can be dynamically determined as

$$\text{ICC} = [x_R - R \sin(\theta_R), y_R + R \cos(\theta_R)]. \quad (7)$$

Also, the mobile robot's position,  $(x'_R, y'_R, \theta'_R)$ , at time  $t + \delta t$ , can be expressed according to the position of the ICC and the angular velocity,  $v_w$ , as follows:



(a) Velocity of a mobile robot.

(b) Representation of robot position.

Fig. 1. Kinematics model of a mobile robot.

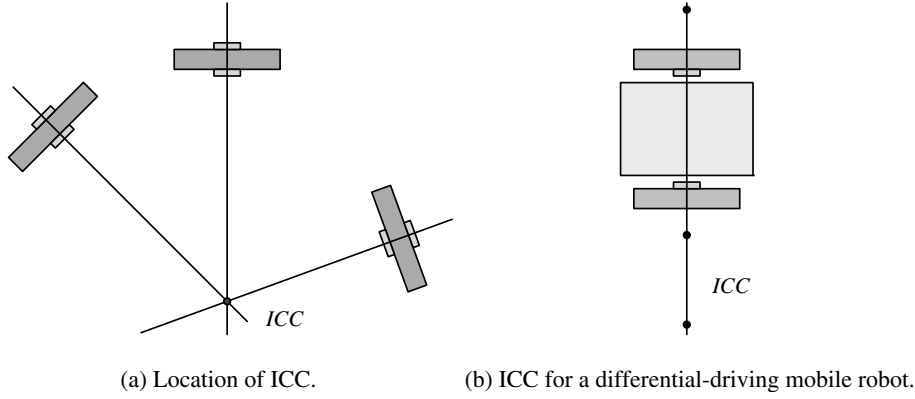


Fig. 2. Location of ICC.

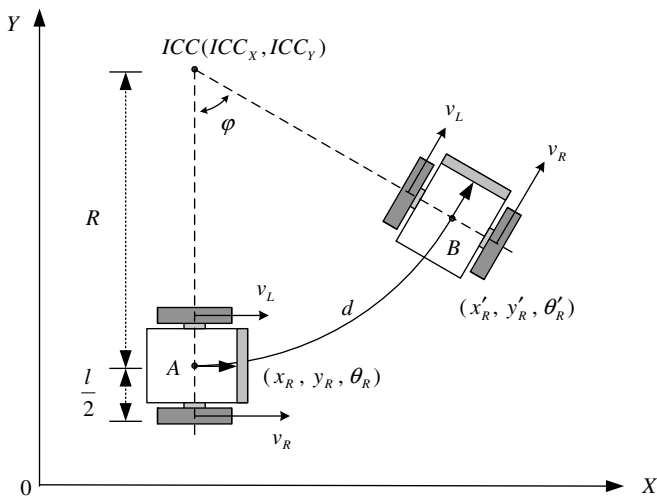


Fig. 3. ICC of a mobile robot.

$$\begin{bmatrix} x'_R \\ y'_R \\ \theta'_R \end{bmatrix} = \begin{bmatrix} \cos(\omega \delta t) & -\sin(\omega \delta t) & 0 \\ \sin(\omega \delta t) & \cos(\omega \delta t) & 0 \\ 0 & 0 & 1 \end{bmatrix} \begin{bmatrix} x_R - ICC_X \\ y_R - ICC_Y \\ \theta_R \end{bmatrix} + \begin{bmatrix} ICC_X \\ ICC_Y \\ v_{\omega} \delta t \end{bmatrix}. \quad (8)$$

Now, the total distance,  $d$ , and the rotation angle,  $\varphi$ , of the mobile robot's movement from location A to B can be obtained as follows:

$$d = \int_t^{t+\delta t} v_1 dt = \int_t^{t+\delta t} \frac{v_L + v_R}{2} dt, \quad (9)$$

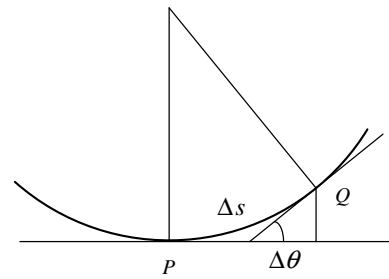
$$\varphi = \frac{d}{R} = \frac{\int_t^{t+\delta t} (v_L + v_R) dt}{l(v_L + v_R)} (v_R - v_L). \quad (10)$$

Using these equations, when the rotation radius, the distance of movement, and the rotation angle of the mobile robot are determined beforehand, the desired linear and angular velocities,  $v_L$ ,  $v_R$ , and  $v_{\omega}$  can be dynamically obtained while the robot is moving in a curved path [16].

### 3. Curvature trajectory

#### 3.1. Curved motion characteristics

The curvature,  $k$ , is defined as the ratio of  $\Delta\theta$  to  $\Delta s$  when a mobile robot is rotating from a point P to Q, as illustrated in Fig. 4. That is, the curvature is defined as [17]

Fig. 4. Curvature,  $\frac{\Delta\theta}{\Delta s}$ .

$$k = \lim_{\Delta s \rightarrow 0} \left| \frac{\Delta\theta}{\Delta s} \right| = \left| \frac{d\theta}{ds} \right|. \quad (11)$$

The rotation radius can be defined as the inverse of the curvature,  $\rho = 1/k$ , (12)

where  $k > 0$ . From Eq. (11), the total traveling distance along the curve,  $\Delta s$ , is the length of the arc and is proportional to the curve-radius. Since the curvature,  $k$ , is inversely proportional to the curve-radius. If  $k = 0$ , then the curve-radius, that is, the rotation radius, becomes infinite. Note that  $k = 0$  implies a straight line, which is a circle of infinite radius.

When the mobile robot is moving along a curved trajectory, the rotation radius has a severe effect on tracking error. Generally, a mobile robot has a smaller chance of error along a straight line ( $k = 0$ ) than on a curved path ( $k \neq 0$ ). Theoretically, a curved trajectory can be calculated with Eqs. (6)–(8), assuming pure-rolling and non-slipping conditions. However, practical driving might result in some divergences from the theoretical values. When a mobile robot is following a curved path, there are combined centrifugal and centripetal forces. The friction force between the surface and the wheels acts as a centripetal force on the ICC and maintains the curved motion of the mobile robot. Under ideal conditions without slippage, the tracking error becomes zero. However, in practical circumstances, there is always a tracking error caused by slippage. The centrifugal force can be formulated as a function of rotation radius,  $R$ , and velocity,  $v$ , [18]

$$F = c \frac{mv^2}{R}, \quad (13)$$

where  $m$  is the mass of the robot and  $c$  is a proportional constant.

Fig. 5 illustrates a driving situation of a mobile robot, starting from A and following a curved path. Under ideal conditions, the estimated position of the robot becomes B1. However, in practical

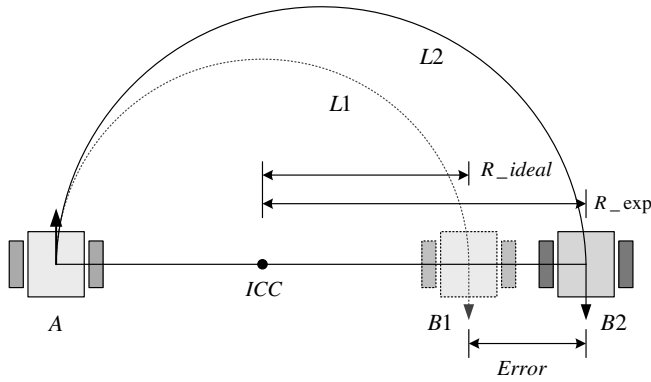


Fig. 5. Driving error of a mobile robot on the curved path.

circumstances, the robot arrives at B2 via a tracking error. There have been many studies conducted to reduce the tracking error caused by a small rotation radius and high traveling velocity. Fig. 6 shows the error characteristics of a real mobile robot, according to the traveling radius and speed [19]. The speed of the right wheel is maintained at a constant, whereas that of the left wheel is changed in order to move the mobile robot in a curved motion. With increases of the left wheel velocity, the tracking error increases as well. Also note that the tracking error increases with a small rotation radius even though the speed is kept constant. From an analysis of Fig. 6, it can be concluded that the tracking error of a mobile robot increases with a smaller rotation radius and with a higher speed while the mobile robot is traveling along a curved path.

### 3.2. Single-curvature trajectory

Fig. 7a and b represent single-curvature and double-curvature trajectories, respectively. The double-curvature trajectory has a

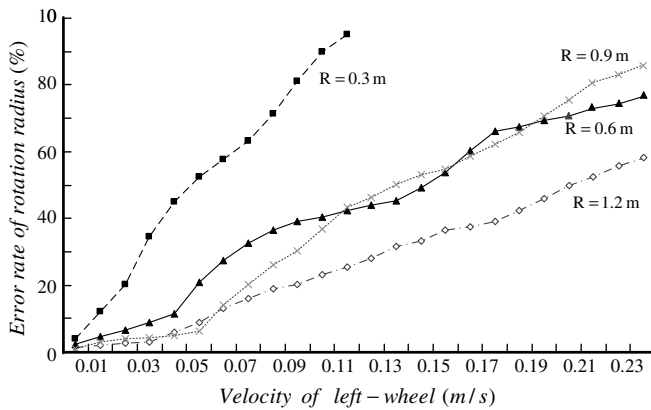


Fig. 6. Driving errors in terms of speed and curve-radius,  $R_0$ .

symmetrical shape with respect to the point of inflection. The single-curvature trajectory keeps the same curvature, while the double-curvature trajectory changes its traveling direction and curvature at the point of inflection. Fig. 7c represents a trajectory that changes its curvature randomly; that is, the points of inflection exist at several locations. While a mobile robot is moving along the trajectory of Fig. 7c, the wheel velocities need to be changed whenever the rotation radius and traveling direction are changed, according to Eq. (7).

For the same travel distance, Fig. 7a shows the biggest rotation radius, whereas the others have various smaller radii. Therefore, it can be predicted that when a mobile robot is traveling along a single-curvature trajectory, it has the least tracking error. Fig. 8 shows the simulation shapes of single-curvature and double-curvature trajectories. Using Eqs. (6)–(11), the rotation radius, traveling distance, rotation angle, and location of the ICC are obtained and are presented in Table 1. The total traveling distances are the same for the single-curvature and double-curvature trajectories. However, the rotation radius of the single-curvature trajectory is two times larger than that of the double-curvature trajectory. Specifically, the rotation radius of the single-curvature trajectory is 5.0 m, whereas that of the double-curvature is 2.5 m, which has the point of inflection at (2.5, 2.5). Close observations of Figs. 6 and 7, led to the expectation that the single-curvature trajectory will have a smaller tracking error than the double-curvature trajectory. Through real experiments, the tracking errors of the single-curvature trajectory and double-curvature trajectory can be compared to each other quantitatively.

The orientation of the mobile robot at the final position is not restricted for the double-curvature trajectory since another point of inflection is needed in order to match the orientation of the mobile robot to the single-curvature trajectory.

## 4. Algorithm for curved trajectory planning

As a typical example for the precise curved motion, the capturing of a moving object by the mobile robot has been demonstrated. This section has proposed an algorithm to produce an optimal trajectory path for capturing a moving object. The proposed algorithm is decomposed into four processes.

### 4.1. Pre-assumptions

Depending on the states of a moving object and a mobile robot, the optimal trajectory for the mobile robot may be different. Therefore, in this paper, an optimal trajectory for a mobile robot has been planned, which considers the restrictions of the motion of the moving object and the mobile robot.

First, the linear velocity of moving object,  $v_{Obj}$ , and angular velocity,  $\frac{d\theta_{Obj}}{dt}$ , are assumed as follows:

$$v_{Obj} = \text{constant}, \quad (14)$$

$$\frac{d\theta_{Obj}}{dt} = 0. \quad (15)$$

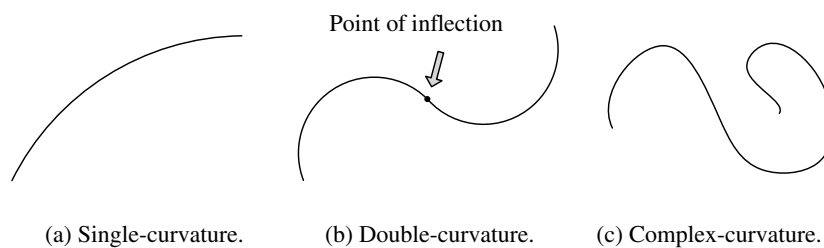


Fig. 7. Types of curvature.

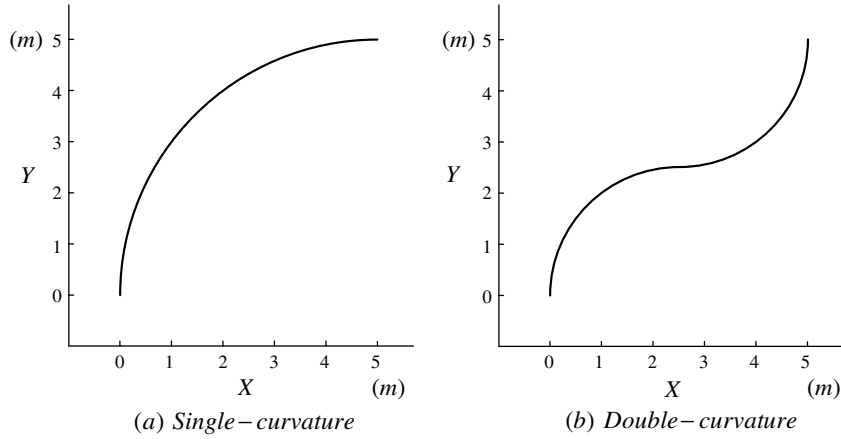


Fig. 8. Single-curvature and double-curvature trajectories.

Table 1

Computed single-curvature and double-curvature trajectories

	Single-curvature trajectory	Double-curvature trajectory
Initial position	$P = (0.0, 0.0, 90^\circ)$	$P = (0.0, 0.0, 90^\circ)$
Final position	$P = (5.0, 5.0, 0.0^\circ)$	$P = (5.0, 5.0, 90^\circ)$
Path distance (m)	7.85 m	7.85 m
Rotation radius (m)	5.0 m	2.5 m
Rotation angle ( $^\circ$ )	$90^\circ$	$\varphi_1 = 90^\circ, \varphi_2 = 90^\circ$
Position of ICC	(5.0, 0.0)	ICC1 = (2.5, 0.0) ICC2 = (2.5, 5.0)

From Eqs. (14) and (15), the motion of the moving object is limited to a straight-line motion in constant velocity from the initial position. It is assumed that the mobile robot is kept static at the beginning, and it should have the same velocity and orientation as the moving object at the capturing moment. For the optimal path planning of a mobile robot, there are two major factors to be considered: the traveling time and the tracking error. If the mobile robot moves rapidly for the minimum driving time, the tracking error will increase in a curved path. Therefore, the conditions for minimum driving time and smallest tracking error can be obtained within the range of the mobile robot's linear velocity and acceleration, which are represented as follows:

$$|v_l| \leq v_{\max} \quad (16)$$

$$\left| \frac{dv_l}{dt} \right| \leq a_{\max}, \quad (17)$$

where  $v_{\max}$  is the maximum allowable linear velocity and  $a_{\max}$  is the maximum allowable acceleration.

For the minimum driving time with a given path, the acceleration of a mobile robot is selected at the maximum speed within the range of allowable acceleration. Also, the maximum velocity of the mobile robot is limited to minimize the tracking error within the maximum allowable range.

#### 4.2. Acquisition of the states of a moving object and mobile robot

Since the optimal path of a mobile robot can be created according to the states of a moving object and mobile robot, the states of the mobile robot and the moving object need to be defined precisely for the successful trajectory planning of the mobile robot. As shown in Fig. 9, the position of a moving object and the mobile robot is defined by two-dimensional  $X-Y$  Cartesian variables,  $x$  and  $y$ , and an orientation variable,  $\theta$ . Then, the orientation of the moving object,  $\theta_{\text{Obj}}$ , is represented as

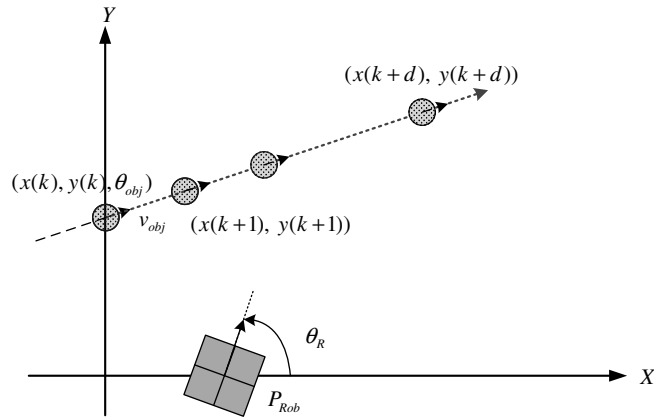


Fig. 9. Initial states of a mobile robot and a moving object.

$$\theta_{\text{Obj}} = \tan^{-1} \left( \frac{y(k+1) - y(k)}{x(k+1) - x(k)} \right). \quad (18)$$

The initial position of moving object,  $P_{\text{Obj}}$ , can be represented as

$$P_{\text{Obj}} = \begin{bmatrix} x(k) & y(k) & \tan^{-1} \left( \frac{y(k+1) - y(k)}{x(k+1) - x(k)} \right) \end{bmatrix}^T. \quad (19)$$

Now, the linear velocity of the moving object,  $v_{\text{Obj}}$ , can be calculated as follows:

$$v_{\text{Obj}} = \frac{\sqrt{(x(k+1) - x(k))^2 + (y(k+1) - y(k))^2}}{t_s} \quad (20)$$

( $t_s$  : sampling period).

The initial position of the mobile robot is represented as

$$P_{\text{Rob}} = \begin{bmatrix} x_R & y_R & \theta_R \end{bmatrix}^T. \quad (21)$$

The mission of the mobile robot requires that it start to capture a moving object with a constant velocity from the stationary initial position. If the mobile robot has the same velocity and orientation with the moving object at the final position, it is natural to assume that the moving object will be captured by the mobile robot.

#### 4.3. Determination of path

According to the initial states of the mobile robot and moving object, either a single-curvature or a double-curvature trajectory is going to be selected. The existence condition for the single curvature trajectory is obtained as  $\alpha = \theta_R - \theta_{\text{Obj}} > 0$ , which is an

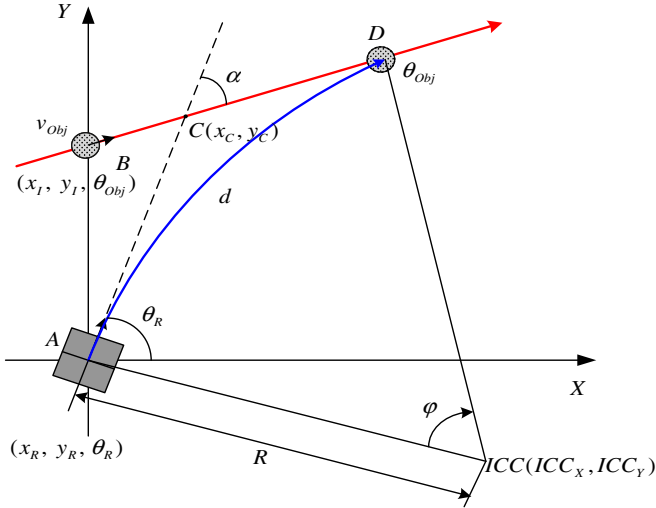


Fig. 10. Single-curvature trajectory.

interesting observation that arose from this research. As shown in Fig. 10, when the mobile robot moves along the single-curvature trajectory, the tracking error from A to D can be minimized, since the slippage of the curved motion can be minimized. As a result, the mobile robot can capture the moving object precisely when it has the same velocity and orientation as the moving object.

If the trajectory and location of the moving object can be estimated accurately, the expected capturing position,  $D(x_D, y_D)$ , is obtained as

$$\sqrt{(x_R - x_C)^2 + (y_R - y_C)^2} = \sqrt{(x_D - x_C)^2 + (y_D - y_C)^2}. \quad (22)$$

In that case, the coordinates of  $C(x_C, y_C)$ , can be obtained from the initial states of a moving object and the mobile robot as follows:

$$\begin{bmatrix} x_C \\ y_C \end{bmatrix} = \begin{bmatrix} \tan(\theta_R) & -1 \\ \tan(\theta_{Obj}) & -1 \end{bmatrix}^{-1} \begin{bmatrix} \tan(\theta_R)x_R - y_R \\ \tan(\theta_{Obj})x_I - y_I \end{bmatrix} \quad (23)$$

where  $(x_I, y_I)$  represents the initial position of the moving object.

The ICC coordinates of the single-curvature trajectory,  $(ICC_X, ICC_Y)$ , and the rotation radius,  $R$ , can be represented as follows:

$$\begin{bmatrix} ICC_X \\ ICC_Y \end{bmatrix} = \begin{bmatrix} -\frac{1}{\tan(\theta_R)} & -1 \\ -\frac{1}{\tan(\theta_{Obj})} & -1 \end{bmatrix}^{-1} \begin{bmatrix} -\frac{1}{\tan(\theta_R)}x_R - y_R \\ -\frac{1}{\tan(\theta_{Obj})}x_D - y_D \end{bmatrix} \quad (24)$$

$$R = \sqrt{(x_R - ICC_X)^2 + (y_R - ICC_Y)^2}. \quad (25)$$

There are some cases where a single-curvature trajectory cannot be produced, since the trajectory depends on the states of the mobile robot and the moving object. As shown in Fig. 11, if the difference between the orientation angles of a moving object and a mobile robot is non-positive ( $\alpha = \theta_R - \theta_{Obj} \leq 0$ ), a single-curvature trajectory cannot satisfy the capturing condition at the final position. In this case, a double-curvature trajectory is selected as the optimal path, instead of a single-curvature one. In such a case, the trajectory of a mobile robot is decomposed into path-1 and path-2. The rotation radius and the coordinates of the ICC are also determined according to the states of the moving object and the mobile robot (see Fig. 12).

From the initial states, the coordinates of ICC1,  $(ICC1_X, ICC1_Y)$ , and ICC2,  $(ICC2_X, ICC2_Y)$ , can be represented as follows:

$$\begin{bmatrix} ICC1_Y \\ ICC2_Y \end{bmatrix} = \begin{bmatrix} -\frac{1}{\tan(\theta_R)}(ICC1_X - x_R) + y_R \\ -\frac{1}{\tan(\theta_{Obj})}(ICC2_X - x_D) + y_D \end{bmatrix}. \quad (26)$$

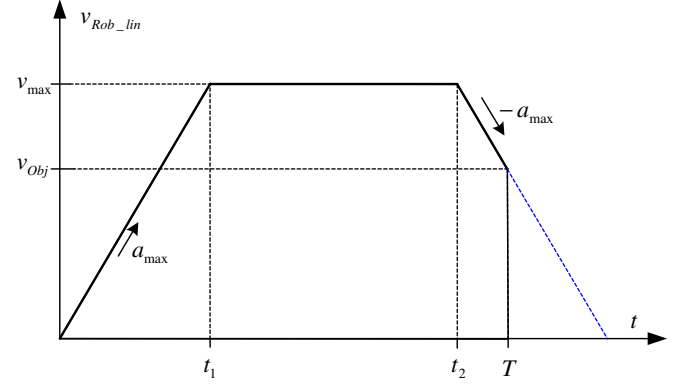


Fig. 11. Double-curvature trajectory.

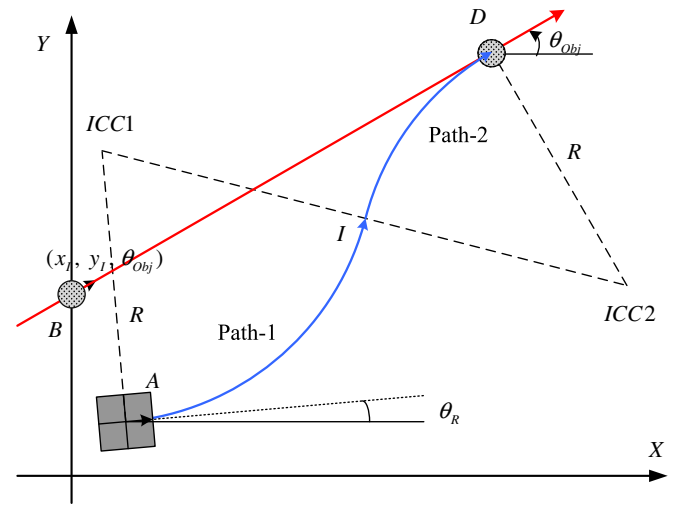


Fig. 12. Velocity profile for the mobile robot.

The rotation radius of Path-1 and Path-2 are selected to be identical to decrease tracking error, and the rotation radius can be represented as

$$\begin{aligned} & \sqrt{(x_D - ICC2_X)^2 + (y_D - ICC2_Y)^2} \\ &= \sqrt{(x_R - ICC1_X)^2 + (y_R - ICC1_Y)^2} \end{aligned} \quad (27)$$

$$R = (1/2) \sqrt{(ICC2_X - ICC1_X)^2 + (ICC2_Y - ICC1_Y)^2}. \quad (28)$$

Note that the direction of the mobile robot is changed at the point of inflection in a double-curvature trajectory.

#### 4.4. Design of velocity profile

The velocity of a mobile robot is determined according to the velocity of the moving object and the driving distance to capture the object. In the single-curvature trajectory, the linear velocity of the mobile robot is divided into three sections: acceleration, uniform velocity, and deceleration.

The linear velocity of the mobile robot can be represented as follows:

$$\begin{cases} v_{Rob\_lin} = a_{max}t & (0 < t < t_1) \\ v_{Rob\_lin} = v_{max} & (t_1 < t < t_2) \\ v_{Rob\_lin} = -a_{max}(t - T) + v_{Obj} & (t_2 < t < T) \end{cases} \quad (29)$$

where  $T$  is the total driving time of the mobile robot.



From the kinematics of a mobile robot, the wheel velocities,  $v_R$  and  $v_L$ , and the angular velocity of the mobile robot,  $\dot{\theta}_R$ , are determined as follows:

$$\begin{bmatrix} v_L & v_R \end{bmatrix} = \begin{bmatrix} \frac{(2R+1)}{2R} v_{Rob\_lin} & \frac{(2R-1)}{2R+1} v_L \end{bmatrix} \quad (30)$$

$$\dot{\theta}_R = 2 \left( \frac{v_L - v_R}{l} \right). \quad (31)$$

For the double-curvature trajectory, two velocity profiles are necessary. That is, at the point of inflection, the mobile robot stops momentarily and changes the velocity profile.

## 5. Experiments

### 5.1. Experimental environment

Experiments were performed in the intelligent robot laboratory (<http://robotics.ee.pusan.ac.kr>). The floor was flat and slippery. The mobile robot used for the experiments was a three-wheeled mobile robot with a two DOF differential driving mechanism. The remote control was implemented using the serial communication channel to the main computer. The mobile robot had a

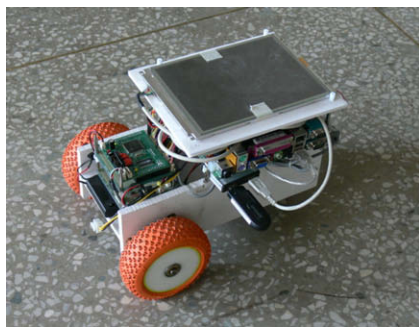


Fig. 13. Mobile robot for the experiments.

**Table 2**  
Hardware specifications of the mobile robot

List	Specification
Size (mm)	320 × 240 × 230 (L × W × H)
Weight	3 Kg
Distance between wheels	200 mm
Radius of wheel	110 mm

DSP320LF2407A controller board to control the motors as shown in Fig. 13. A 10 bits encoder was installed on each wheel of the mobile robot and the sampling period for the moving object was 1/30 second. The hardware specifications of the mobile robot are summarized in Table 2.

### 5.2. Experiments to show the superiority of a single-curvature trajectory

In the first two experiments, the same mobile robot moved on the single-curvature and double-curvature trajectories to capture a moving object as shown in Fig. 14. The tracking errors are measured and compared in Fig. 15. The computed single-curvature and double-curvature trajectories shown in Table 1 were utilized to capture the moving object.

As is illustrated in Fig. 15, the tracking error for the double-curvature trajectory increases very rapidly while that of the single-trajectory increases slowly. Through these experiments, it is concluded that a single-curvature trajectory is the best for the precise tracking operation, unless it is impossible.

### 5.3. Experiments for the capturing trajectory

The second experiments were performed to show the effectiveness of the proposed algorithm to capture a moving object. In the experiments, the maximum allowable acceleration was set to 0.1 m/s<sup>2</sup> and the moving object's linear velocity was assumed to

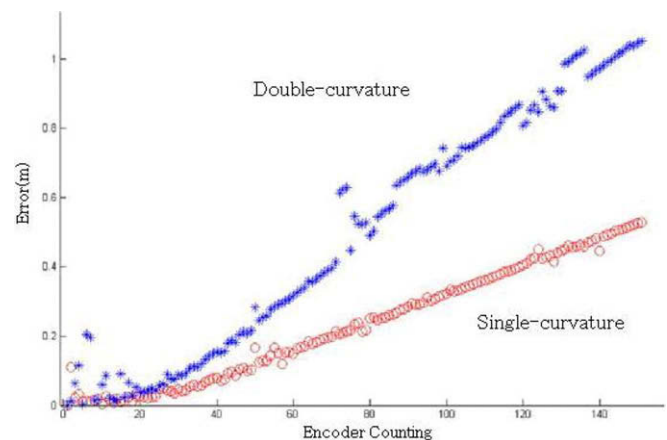
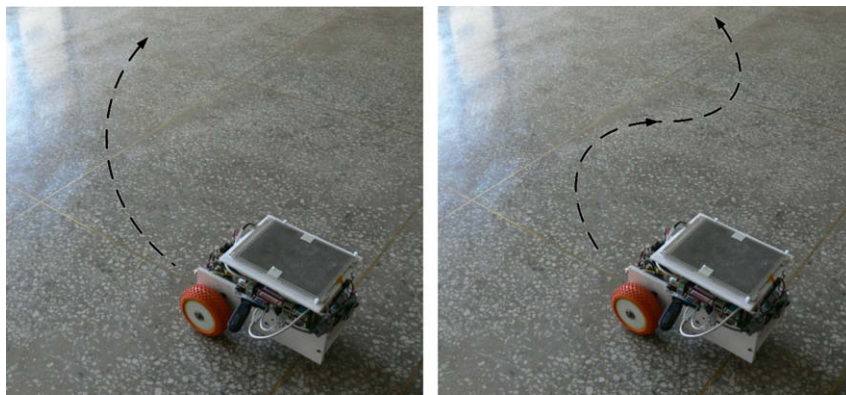


Fig. 15. Comparison of tracking errors.



(a) Single-curvature driving.

(b) Double-curvature driving.

Fig. 14. Comparison of single- and double-curvature driving.

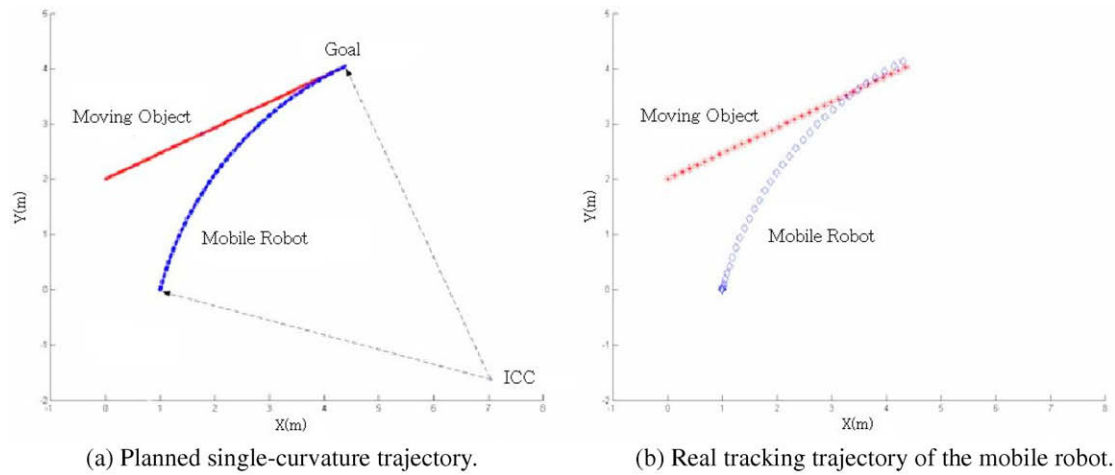


Fig. 16. Single-curvature trajectory for capturing the moving object.

be constant at 0.3 m/s. The sampling period was 0.1 second. Based on the proposed algorithm, a single-curvature trajectory was planned to capture the moving object as shown in Fig. 16a. The experimental results with the single-curvature trajectory are illustrated in Fig. 16b, and the specifications and experimental results of the single-curvature trajectory are summarized in Table 3.

When the single-curvature trajectory is not available (when  $\alpha = \theta_R - \theta_{Obj} \leq 0$ ), a double-curvature trajectory is selected as the optimal trajectory instead of a single-curvature trajectory to capture the moving object. Fig. 17a illustrates the path that a mobile

robot should follow the moving object to capture it along a double-curvature trajectory. The experimental results with the double-curvature trajectory are illustrated in Fig. 17b, and the specifications and experimental results of the double-curvature trajectory are summarized in Table 4.

Through these experiments, it is confirmed again that the double-curvature trajectory has a larger tracking error than the single-curvature trajectory. Even though the trajectory generation processes are not illustrated in this section, the algorithm explained in Section 4 plays an important role for successful tracking and capturing.

**Table 3**  
Specifications and experimental results of the single-curvature trajectory

	Single-curvature trajectory	Error
The position of moving object	(0, 2, 25°)	–
Initial position of mobile robot	(1, 0, 75°)	–
ICC coordinates	(7.04, –1.61)	–
<i>Capturing position</i>		
Computed	(4.35, 4.03)	0.12 m
Real	(4.30, 4.14)	
<i>Rotation radius</i>		
Computed	6.26 m	0.35 m
Real	6.61 m	

**Table 4**  
Specifications and experimental results of double-curvature trajectory

	Double-curvature trajectory	Error
Position of moving object	(0, 2, 30°)	–
Position of mobile robot	(1, 0, 5°)	–
ICC coordinates	(0.74, 2.99), (6.71, 2.41)	–
<i>Capturing position</i>		
Computed	(5.21, 5.01)	0.3068
Real	(5.31, 4.70)	
<i>Rotation radius</i>		
Computed	3 m	0.47
Real	R1 = 3.47, R2 = 3.19	

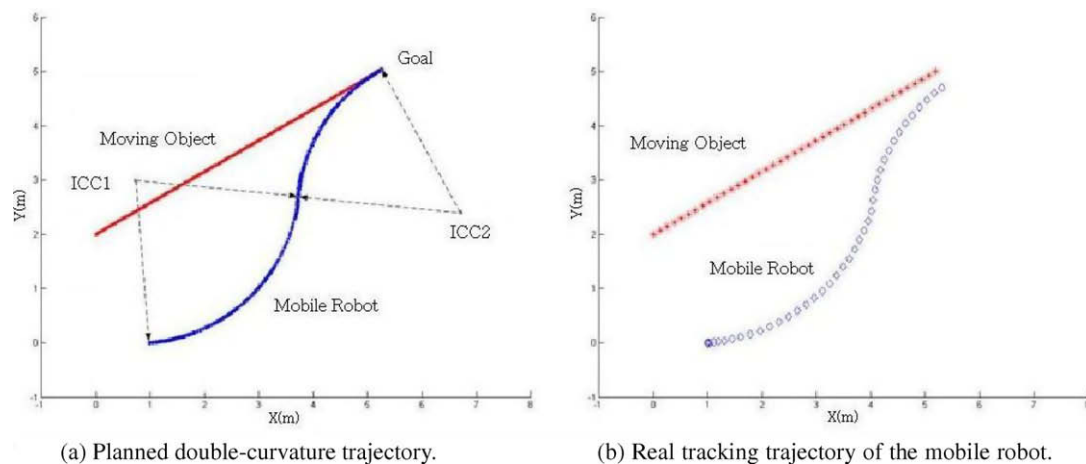


Fig. 17. Double-curvature trajectory for capturing the moving object.



## 6. Conclusion

In this paper, a new algorithm for the optimal trajectory planning of a differential driving mobile robot has been proposed. Among the many factors that cause tracking errors for the mobile robot, the curvature of the path is thoroughly analyzed in this paper, since it can be selected without effecting the task execution. This study demonstrates the optimality of a single-curvature trajectory for a precise curved motion. An example of the precise-curved motion, the capturing of a moving object, is illustrated by real experiments. The superiority of the single-curvature trajectory has been verified based on both theoretical observations and real experiments. Since mobile robots with dead-reckoning sensors can only aggregate the position estimation error while they are navigating, an error correction algorithm is necessary to support precise and prompt control. Frequent error correction processes degrade the driving performance critically and may cause unstable operations. Providing a trajectory which causes less error is very effective for the precise and fast-curved tracking motion of a differential driving mobile robot. To improve the driving accuracy of the mobile robot, intelligent position estimation schemes and driving control algorithms will have to be developed further in future research.

## Acknowledgement

This work was supported in part by MIC and IITA through IT Leading R&D Support Project.

## References

- [1] Ge SS, Cui YJ. New potential functions for mobile robot path planning. *IEEE Trans Robot Autom* 2000;16(5):615–20.
- [2] Pathak Kaustubh, Agrawal Sunil K. An integrated path-planning and control approach for nonholonomic unicycles using switched local potentials. *IEEE Trans Robot* 2005;21(6):1201–8.
- [3] Fan Xiaoping, Luo Xiong, Yi Sheng, Yang Shengyue, Zhang Heng. Optimal path planning for mobile robots based on intensified ant colony optimization algorithm. *Proc IEEE Int Conf Robotic Intell Syst* 2003;1(Oct.):131–6.
- [4] Georgiev Atanas, Allen Peter K. Localization methods for a mobile robot in urban environments. *IEEE Trans Robot* 2004;20(5):851–64.
- [5] Garulli Andrea, Vicino Antonio. Set membership localization of mobile robots via angle measurements. *IEEE Trans Robot Autom* 2001;17(4):450–63.
- [6] Liu Hugh HS, Pang Grantham KH. Accelerometer for mobile robot positioning. *IEEE Trans Ind Appl* 2001;37(3):812–9.
- [7] Chwa Dongkyoung. Sliding-mode tracking control of nonholonomic wheeled mobile robots in polar coordinates. *IEEE Trans Control Syst Technol* 2004;12(4):637–44.
- [8] Chang Wen-Chung, Lee Shu-An. Autonomous vision-based pose control of mobile robots with tele-supervision. In: *Proc IEEE Int Conf on Control Appl*; September 2004. p. 1049–54.
- [9] Li Tzuu-Hseng S, Chang Shih-Jie, Tong Wei. Fuzzy target tracking control of autonomous mobile robots by using infrared sensors. *IEEE Trans Fuzzy Syst* 2004;12(4):491–501.
- [10] Wei Shangming, Zefran Milo. Smooth path planning and control for mobile robots. In: *Proc IEEE Proc Network Sens Control*; March 2005. p. 894–9.
- [11] Choi HR, Ryew SM. Robotic system with active steering capability for internal inspection of urban gas pipelines. *Mechatronics* 2002;12(5):713–36.
- [12] Hague T, Tillett ND. Navigation and control of an autonomous horticultural robot. *Mechatronics* 1996;6(2):165–80.
- [13] Fukao Takanori, Nakagawa Hiroshi, Adachi Norihiko. Adaptive tracking control of a nonholonomic mobile robot. *IEEE Trans Robot Autom* 2000;16(5):609–15.
- [14] Dixon WE, de Queiroz MS, Dawson DM, Flynn TJ. Adaptive tracking and regulation of a wheeled mobile robot with controller/update law modularity. *IEEE Trans Control Syst Technol* 2004;12(1):138–47.
- [15] Mutambara Arthur GO, Durrant-Whyte Hugh F. Estimation and control for a modular wheeled mobile robot. *IEEE Trans Control Syst Technol* 2000;8(1):35–46.
- [16] Barfoot Timothy D, Clark Christopher M, Rock Stephen M, D'Eleuterio Gabriele M. Kinematic path-planning for formations of mobile robots with a nonholonomic constraint intelligent. *Proc IEEE/RSJ Int Conf Robot Syst* 2002;3(September):2819–24.
- [17] Fraichard Thierry, Scheuer Alexis. From Reeds and Shepp's to continuous-curvature paths. *IEEE Trans Robot* 2004;20(6):1025–35.
- [18] Scheuer A, Fkaichard Th. Continuous-curvature path planning for car-like vehicles. *Proc IEEE/RSJ Int Conf Intell Robot Syst* 1997;2(September):997–1003.
- [19] NoYong-Jun. A study on the reduction of navigation error for curvilinear navigation of mobile robot using neural network, Master's thesis. Chonnam National University, Korea; 2002.